International Journal of Research in Advent Technology, Vol.6, No.6, June 2018
E-ISSN: 2321-9637
Available online at www.ijrat.org

Synthesis and Investigation on structural and optical properties of SnO_2 nanocrystals

P. Gomathy[1], S. Meenakshi Sundar[2]
Reg. No: 9274[1], Associate Professor[2],
PG and Research Department of Physics, Sri Paramakalyani College, Alwarkurichi - 627 412, Tamilnadu, India[1,2].
Affiliated to Manonmaniam Sundaranar University, Abishekapatti, Tirunelveli-627 012, TamilNadu, India[1,2].
Email:gomsnatarajan.pons@gmail.com[1], smsun_1964@yahoo.co.in[2]

Abstract-The present investigation reports the characterization of nanocrystalline tin oxide synthesized by microwave assisted solvothermal method using urea as catalyst and ethylene glycol as solvent. The prepared sample is annealed at different temperatures from 300^0 C to 700^0 C for 1 hour for the formation of SnO_2 crystalline phase. The structural features have been studied using XRD, FTIR, TEM and SAED pattern. The phase and crystalline structure were confirmed with the help of X-ray diffraction and FTIR spectroscopy. The crystalline size was evaluated from XRD and found to range from 4 to 17 nm. Based on the recorded FTIR spectrum of SnO_2, the IR band due to SnO_2 vibrations was observed at 621 cm^{-1}. The formation of small sized spherical nanoparticles of the diameter of about 14-45 nm was illustrated by transmission electron microscope results. The optical properties have been analysed by PL studies. The intercept of the energy axis in Tauc Plots gives the direct measurement of the band gap (E_g). The photoluminescence PL measurement for the tin oxide nanoparticles annealed at 500^oC indicated that there are two stable emission peaks centered at wavelengths 568 nm and 374 nm by oxygen vacancies.

Index Terms-tin oxide nanoparticles, XRD, TEM, Photoluminescence.

1. INTRODUCTION

Synthesis of nanomaterials, with controlled morphology, size, chemical composition, crystal structure and in large quantity, is a challenge in nanotechnological applications. The various geometrical morphologies of nanomaterials such as nano tubes [1,2], cages [3], cylindrical wires [4,5], rods [6], biaxial cables [7], ribbons or belts [8], and sheets [9] have been produced with the peculiar properties. The experimental methods to synthesize nanoparticles such as chemical precipitation [10], microwave technique [11], combustion route [12], sol–gel [13], solvothermal [14], hydrothermal [15], sonochemical [16] and mechanochemical [17] have been reported with different sizes and shapes.

Tin oxide (SnO_2) with a wide band gap of 3.6 eV is observed as one of the potential materials for gas sensors, solar cells, transparent electrodes and field effect transistors [18–23]. The large direct bandgap and a high exciton binding energy (130meV) of SnO_2 are favourable for room-temperature UV applications. The research on optical studies on wide band gap semiconducting materials have been done. But there have been only rare investigations of SnO_2 optical properties. This is due to the even-parity symmetry of the conduction-band minimum and the valence-band maximum in SnO_2, which bans the band-edge radiative transition.

The carrier concentration of n-type tin oxide semiconductor is very high (up to 6 x 10^{20} cm^{-3}) [24]. Nowadays tin oxide is used in wide range of application such as lithium - ion batteries, [25,26], catalysts for oxidation of organics, and electrodes in solid state ionic devices, because of its peculiar properties such as chemically inert, mechanically hard and thermally heat resistant [27,28]. The success in many of its technological applications depends on the crystalline SnO_2 with a uniform nanosize pore structure [29]. The progress in research towards tin oxide nanomaterials with high sensitivity, excellent selectivity, quick response and recovery behavior to gases have increased.

2. MATERIALS AND METHODS

Tin oxide powder was prepared by following the microwave assisted solvothermal method. Analytical grade tin II chloride ($SnCl_4{\cdot}2H_2O$) was used as starting material for the synthesis of SnO_2 nanopowder. Urea and ethylene glycol were used as catalyst and as solvent respectively. Initially at room temperature, tin(II) chloride and urea were dissolved in ethylene glycol by constant stirring for 2 hours in a magnetic stirrer. The microwave power was set to 650 W and operated at the rate of 2 min per cycle and cooled between the intervals until the precipitate was formed. The resulting precipitate was washed with double distilled water and dried. Again, the dried powders were washed with acetone to remove the impurities, and then annealed at 500° C for 1 h in air atmosphere. The properties of the prepared samples are investigated using XRD, TEM-SAED, FTIR, UV-Vis, and PL studies.

3. RESULTS AND DISCUSSION

3.1. *Phase Analysis*

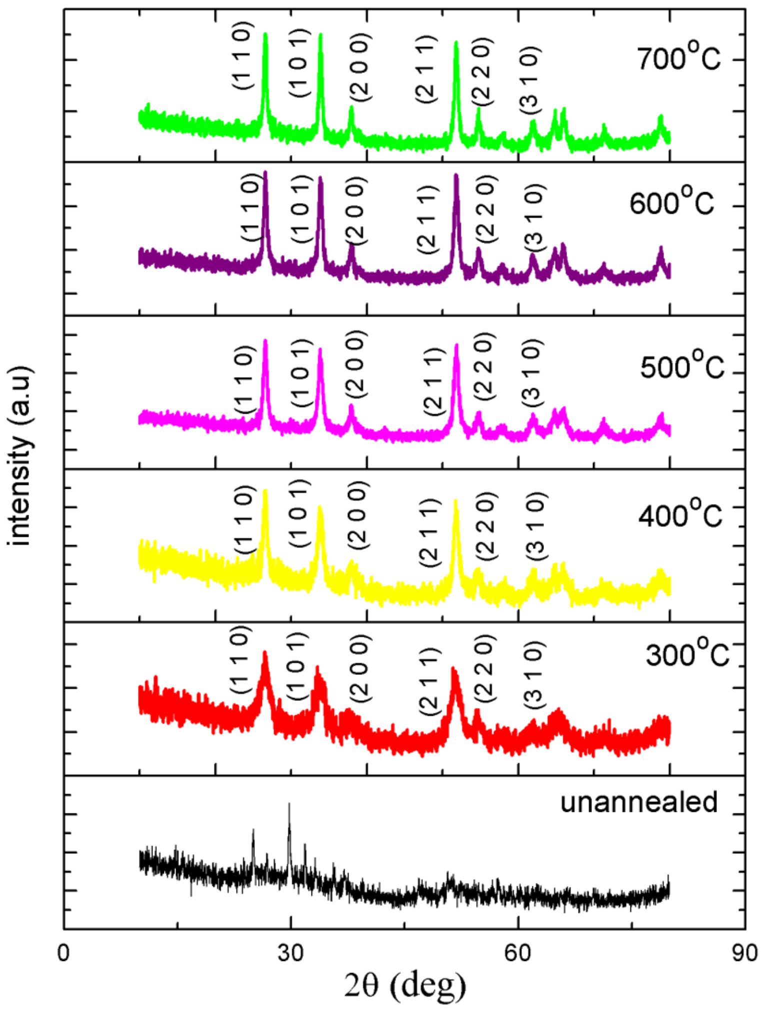

Figure 1. XRD patterns of SnO_2 samples annealed at different temperatures

Figure 1 shows X-ray diffraction (XRD) patterns of SnO_2 nanoparticles annealed at different temperatures from 300^0C to 700^0C respectively. The unannealed sample shows the amorphous structure. The peak orientations in the planes (110), (101), (200), (211), (220), (310), (112) and (301) clearly indicate the effective growth of the nanostructure. The present peaks in the spectra confirm the polycrystalline nature of the nanostructures, which were identified to create of tetragonal rutile crystal structure of SnO_2 (JCPDS card No. 77-0451) and no other diffraction peak is noticed, which proves that the nanoparticles are SnO_2 with a single phase. The crystalline nature of SnO_2 nanoparticles is analysed by narrow XRD peaks. The intensity of XRD peak is increased when the calcination temperature is increased It signifies the progress of crystallinity. The small crystallite size is understood by the broadening of the width of the prepared samples' Bragg peaks in XRD spectrum. As the annealing temperature increases from 300^0C to 700^0C, the intensity of the peaks gets increased, where as the FWHM gets reduced. The nanocrystalline powders can be formed due to the decrease in peak broadenings and sharpening of the intensities of the peaks with the increasing temperatures.

Crystalline size "D" was obtained by the measurement of the broadening of diffraction lines and by applying the Debye-Scherrer formula [30]

$$D= 0.9\,\lambda / (\beta \cos\theta)$$

where λ is the wavelength of Cu Kα radiations (1.5418 A°), β is the full-width at half-maximum of the peaks corresponding to the plane, and θ is the angle obtained from 2θ value corresponding to a maximum intensity peak in XRD pattern. The crystalline size of the obtained SnO_2 particles was varying from 4 to 17nm for the annealing temperature from 300^0C to 700^0C. Table 1 shows the various structural parameters of our prepared SnO_2 samples.

Table 1. Particle size, lattice parameter and cell volume of SnO_2 nanoparticles at different sintering temperatures

Sintering Temperature °C	Crystallite Size (nm)	Lattice Parameters (A°)		c/a	Cell Volume (A^3)
		a=b	c		
300	04.25	4.7417	3.2226	0.6796	72.456
400	11.37	4.7361	3.1860	0.6727	71.465
500	12.57	4.7354	3.1855	0.6727	71.431
600	12.87	4.7321	3.1828	0.6726	71.272
700	17.00	4.7346	3.1838	0.6725	71.369

3.2. *Functional group analysis*

The size of the peaks in the FTIR spectrum directly indicates the amount of material present and also represents the defect or surface vacancies in the crystalline structure of the surface layer. FT-IR spectrum of SnO_2 nanoparticles treated at 500°C and 600°C is shown in Figure 2.

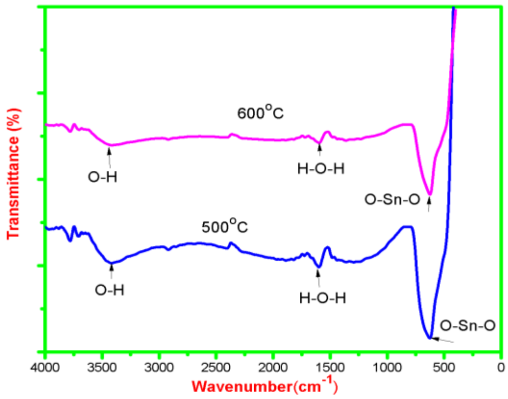

Figure 2. FT-IR spectrum of SnO_2 nanoparticles annealed at 500°C and 600°C

The intense and broad bands at 3420 cm^{-1} and 1611 cm^{-1} have been assigned as the O–H vibration in absorbed water on the sample surface [31]. Usually, the FTIR samples are kept and ground in air. The nanostructured materials are having the high surface area. Due to this important property of the nanoparticles, the surface area results in rapid adsorption of water from the atmosphere. The broad bands between 400 and 800 cm^{-1} are credited to the framework vibrations of the O–Sn–O bond in SnO_2 [32]. The peak appeared at 621 cm^{-1} relates to the O–Sn–O bridge functional groups of SnO_2. This proves the existence of SnO_2 which is in crystalline phase. This is in accord with the results of the XRD analysis.

3.3. *TEM study*

The direct observation of TEM also verifies the existence of the tin oxide nanocrystals in our sample. Figure 3 and Figure 4 show the SAED pattern and TEM image of the SnO_2 nanoparticles annealed at 500°C. The darker regions of Figure 4.9 (b) represent the tin oxide nanocrystals. Moreover, we can view the appearance of some lattice fringes in the darker regions. SnO_2 grains have agglomerated spherical morphology with a particle size of 14-45 nm estimated by TEM micrographs. The electron diffraction rings formed by the tin oxide nanocrystals are shown in the corresponding SAED pattern. The ring pattern is indexed to the tetragonal rutile phase of tin oxide [33] according to JCPDS file number of 77-0451. The highly crystalline nature of our sample is indicated by the intense white dots appeared in continuous ring pattern of the selected-area-electron-diffraction (SAED) pattern (Figure 3). The lattice spacing between the fringes in SAED pattern is matched with the lattice spacing values of the (110), (101), (200) and (211) planes observed in the XRD pattern and is shown in Table 2.

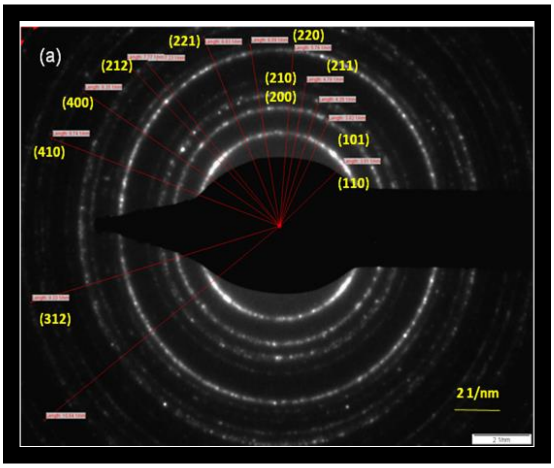

Figure 3. SAED Pattern of SnO_2 nanoparticles

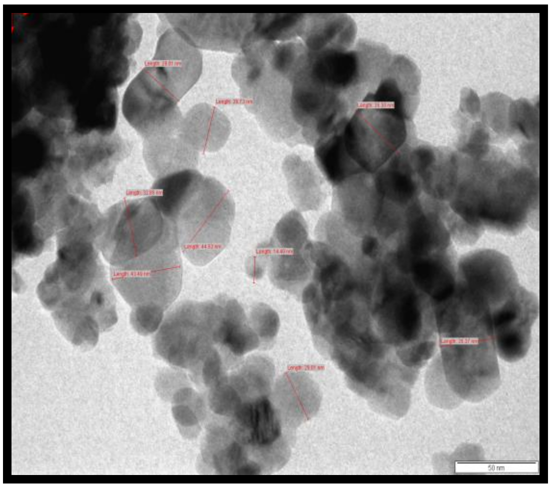

Figure 4. TEM image of SnO_2 nanoparticles

Table 2. Interplanar distance of SnO_2 nanoparticles annealed at 500 °C

Planes (hkl)	d values from XRD (A^0)	d values from TEM (A^0)
(110)	3.3593	3.322
(101)	2.6520	2.617
(200)	2.3754	2.347
(211)	1.7694	1.736

3.4. *Bandgap Analysis*

SnO_2 nanoparticles annealed at 500℃ were subjected to optical absorption measurement. The variation of the optical absorbance with the wavelength of the SnO_2 nanoparticles is shown in Figure 5. The optical absorption coefficient is calculated in the wavelength range of 300 – 800 nm. It is observed from our UV-Vis measurements that the absorption band has been acquired at a shorter wavelength. Our prepared sample is good crystalline nanocrystal with less surface defects and it is homogeneously distributed. This is evaluated by the sharp rise of the spectrum at the absorption edge [34]. If the size of the nanoparticles is reduced, the surface to volume ratio becomes high. This produces the surface related defects in the nanocrystals. Due to the quantum confinement of the nanoparticles, the absorption spectrum gets broaden. Our UV-Vis absorption spectrum of SnO_2 nanoparticles shows the absorbance edge at 310 nm (E_g=4eV), which agrees well with the reported value of 312 nm [35]. The better crystallinity and lower defect density for the synthesized nanoparticles are also specified by the significant decrease in the transmittance for SnO_2 nanocrystallites near the band edge.

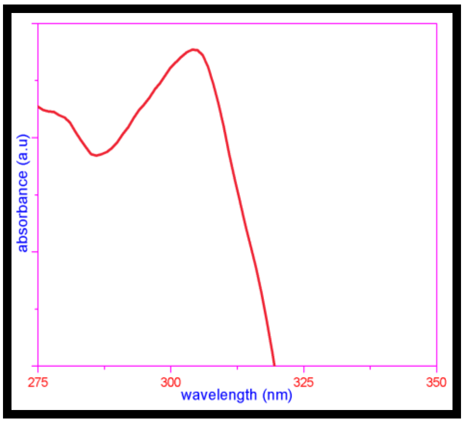

Figure 5. UV-VIS absorption spectrum of SnO_2 nanoparticles annealed at 500^{o}C

The optical band gap energy (E_g) is the important parameter of semiconductor nanoparticles. The optical absorption relates the absorption coefficient α with the photon energy hν for the direct allowed transition as [36]

$$\alpha h\nu = A(E_g - h\nu)^{1/2}$$

in which hν is the photon energy, E_g is the apparent optical band gap, A is a constant characteristic of the semiconductor, and α is the absorption coefficient. The above equation is referred as tauc relation which is used to determine the energy value of direct band gap of the semiconductor. Figure 6 shows the graph of $(\alpha h\nu)^2$ versus photon energy hν for SnO_2 nanoparticles annealed at the temperature 500°C. A plot of $(\alpha h\nu)^2$ versus hν shows intermediate linear region and the extrapolation of the linear part is used to calculate the value of E_g from intersect with hν axis at α = 0. The intercept value on the energy axis has been found to be 4 eV for the sample. This optical band gap is larger than the value of 3.62 eV for bulk SnO_2 due to the quantum size effect [37].

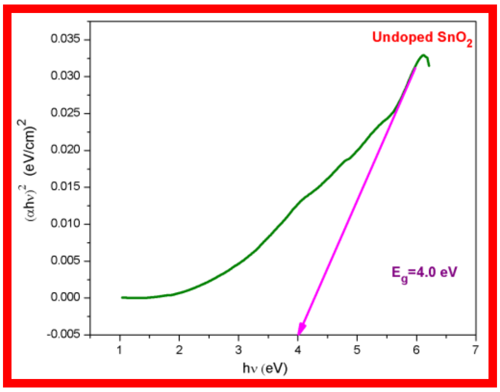

Figure 6. Tauc plot for SnO_2 nanoparticles annealed at 500°C.

3.5. *Photoluminescence Studies*

PL measurements have been carried out at room temperature to investigate the potential of the luminescent properties of SnO_2 nanoparticles, Figure 7 demonstrates the emission spectrum of our prepared sample.

Generally, the most common defects occurred in oxides are the oxygen vacancies and they usually act as the radiative centers in luminescence method. The defect levels may be formed in the band gap of SnO_2 nanocrystals due to the intrinsic defects such as oxygen defects. It causes the electrons to trap from the valence band to make a contribution to the luminescence. Our synthesized SnO_2 nanoparticles exhibit a near-UV emission peak at 374 nm, by the contribution of oxygen vacancies and defects in the SnO_2 nanoparticles [38,39]. The direct recombination of a conduction electron in the Sn 4d band with a hole in the O 2p valence band may not produce the luminescence band observed at 568 nm. In our PL emission spectrum, the broad luminescence band between 500 and 600 nm may be produced by the defect levels in the band gap of SnO_2 nanoparticles at room temperature which is already mentioned in the earlier reports [40–44].

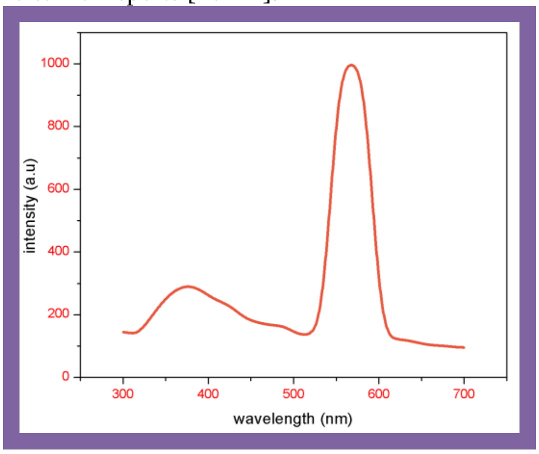

Figure 7. PL emission spectrum of sample annealed at 500°C

4. Conclusion

In summary, we have successfully prepared SnO_2 nanoparticles by microwave assisted solvothermal method. The as-synthesized SnO_2 nanoparticles were annealed at 300– 700 ˚C for 1 hour in ambient conditions. We have made the following observations by performing several experiments on prepared samples.

i) The XRD analysis indicated that the as synthesized and annealed SnO_2 nanoparticle samples demonstrate the single phase nature and there is no impurity phases. The grain growth occurs as the increment in the annealing temperature. This shows the effective crystalline nature of the nanoparticles

ii) It is confirmed from TEM images that the nanosize particles are in our investigated samples. We also observe that synthesized SnO_2 nanoparticles are spherical in shape and crystalline nature is further confirmed by SAED images.

iii) The optical band gap of the nanoparticles depends on quantum confinement. Oxygen vacancies play an important part in determining the optical properties of synthesized and annealed SnO_2 nanoparticles. Our sample annealed at 500°C exhibit the strong emissions at

374nm and 568 nm, due to the contribution of oxygen vacancies and crystal defects.

Acknowledgements

Authors are very much thankful to the management of Sri Paramakalyani College, Alwarkurichi, Tamilnadu, India for their constant support.

REFERENCES

[1]. Remskar, M.; Mrzel, A.; Skraba, Z.; Jesih, A.; Ceh, M.; Demsar, J.; Stadelmann, P.; Levy, F.; Mihailovic. (2001): Self-assembly of subnanometer-diameter single-wall MoS_2 nanotubes. D. Science, 292(5516), 479-481.

[2]. Jie Lin, Jin-Myoung Lim, Duck Hyun Youn, Kenta Kawashima, Jun-Hyuk Kim, Yang Liu, Hang Guo, Graeme Henkelman, Adam Heller and Charles Buddie Mullins. (2017): Self-Assembled Cu–Sn–S Nanotubes with High (De)Lithiation Performance, ACS Nano, 10.1021/acsnano.7b05294, 11, 10, (10347-10356).

[3]. Tenne, R.; Homyonfer, M.; Feldman, Y. (1998): Nanoparticles of Layered Compounds with Hollow Cage Structures (Inorganic Fullerene-Like Structures), Chem. Mater. 10(11), 3225- 3238.

[4]. Pan, Z. W.; Dai, Z. R.; Ma, C.; Wang, Z. L. (2002): Molten Gallium as a Catalyst for the Large-Scale Growth of Highly Aligned Silica Nanowires J. Am. Chem. Soc. 124(8), 1817-1822.

[5]. Krishna Nama Manjunatha, Shashi Paul. (2017): In-situ catalyst mediated growth and self-doped silicon nanowires for use in nanowire solar cells, Vacuum, 139, (178).

[6]. Manna, L.; Scher, E. C.; Alivisatos. (2000): Synthesis of Soluble and Processable Rod-, Arrow-, Teardrop-, and Tetrapod-Shaped CdSe NanocrystalsA. P. J. Am. Chem. Soc. 122[51], 12700-12706.

[7]. Wang, Z. L.; Dai, Z. R.; Gao, R. P.; Bai, Z. G., Gole. (2000): Side-by-side silicon carbide–silica biaxial nanowires: Synthesis, structure, and mechanical propertiesJ. L. Appl. Phys. Lett. 77, 3349-3351.

[8]. Shi, W.; Peng, H.; Wang, N.; Li, C. P.; Xu, L.; Lee, C. S.; Kalish, R.; Lee. (2001): Springs, Rings, and Spirals of Rutile-Structured Tin Oxide Nanobelts, S. T. J. Am. Chem. Soc. 123, 11095-11096.

[9]. Yourong Tao, Xingcai Wu, Wei Wang and Jianan Wang. (2015): Flexible photodetector from ultraviolet to near infrared based on a SnS 2 nanosheet microsphere film , *J.Mater.Chem.C*, 10.1039/C4TC02325 K, **3**, 6, (1347-1353).

[10]. Yu Dabin, Wang Debao, Yu Weichao, Qian Yitai. (2004): Synthesis of ITO nanowires and nanorods with corundum structure by a co-precipitation-anneal method, Mater Lett. 58 : 84–87.

[11]. Krishnakumar,T.;Jayaprakash,R.;Pinna,N.; Singh VN, Mehta BR, Phani AR. (2009): Microwave-assisted synthesis and characterization of flower shaped zinc oxide nanostructures, Mater Lett. 63 : 242–245.

[12]. Fraigi LB, Lamas DG, Walsoe de Reca NE. (2001): Comparison between two combustion routes for the synthesis of nanocrystalline SnO_2 powders Mater Lett. 47:262–266.

[13]. Korosi L, Papp S, Meynen V, Cool P, Vansant EF. (2005): Dekany Preparation and characterization of SnO_2 nanoparticles of enhanced thermal stability: The effect of phosphoric acid treatment on $SnO_2{\cdot}nH_2O$ I. Colloids Surf A: Physicochem Eng Asp. 268:147–154.

[14]. Han Zhaohui, Guo Neng, Li Fanqing, Zhang Wanqun, Zhao Huaquiao, Qian Yitai. (2001): Solvothermal preparation and morphological evolution of stannous oxide powders, Mater Lett. 48:99–103.

[15]. Sakai Go, Baik Nam Seok, Miura Norio, Yamazoe Noboru. (2001): Gas sensing properties of tin oxide thin films fabricated from hydrothermally treated nanoparticles: Dependence of CO and H2 response on film thickness Sens Actuators B. 77: 116–121.

[16]. Hu Xian Luo, Zhu Ying-Ji, Wang Shi-Wei. (2004): Sonochemical and microwave-assisted synthesis of linked single-crystalline ZnO rods, Mater Chem Phys. 88:421–426.

[17]. Cukrov LM, Mc Cormick PG, Galatsis K, Wlodarski W. (2007): Gas sensing properties of nanosized tin oxide synthesised by mechanochemical processing, Sens Actuators B.77: 491–495.

[18]. Lettieri,S.; Setaro,A.; Baratto,C.; Comini,E.; Faglia,G.; Sberveglieri,G.; Maddalena,P. (2008): On the mechanism photoluminescence quenching in tin oxide nanowires by NO_2 adsorption, New J. Phys. 10 (043013).

[19]. Lettieri,S.; Causa,M.; Setaro, A.; Trani, F.; Barone, V.; Ninno,D.; Maddalena,P. (2008): Direct role of surface oxygen vacancies in

visible light emission of tin dioxide nanowires, J.Chem. Phys. 129 (244710).

[20]. Reddy,A.S.; Figueiredo,N.M.; Cavaleiro, A. (2012): Nanocrystalline SnO2 and Au:SnO2 thin films prepared by direct current magnetron reactive sputtering, Vacuum, 86, 1323-1327.

[21]. He,H.; Wu,T.H.; Hsin,C.L.; Li,K.M.; Chen, L.J.; Chueh,Y.L.; Chou,L.J.; Wang,Z.L. (2006); Beaklike SnO2 nanorods with strong photoluminescent and field-emission properties, Small, 2 116-120.

[22]. Ferrere,S.; Zaban,A.; Gsegg,B.A. (1997): Dye Sensitization of Nanocrystalline Tin Oxide by Perylene Derivatives, J. Phys. Chem. B 101, 4490-4493.

[23]. Mathur,S.; Barth,S.; Shen,H.; Pyun,J.C.; Werner,U.(2005):Size-dependent photoconductance in SnO_2 nanowires, Small 1, 713-717.

[24]. Grosse, P.; Schmitte,F.J.; Frank,G.; Kostlin,H. (1982): Preparation and growth of SnO_2 thin films and their optical and electrical properties, Thin Solid Films 90 309–315.

[25]. Zuo-Yan,P.; Zhong,S.; Mei-Lin,L.(2000): Mesoporous Sn–TiO2 composite electrodes for lithium batteries, Chem. Commun. 21 2125–2126.

[26]. Ferrere,S.; Zaban,A.; Gregg,B.A. (1997): Dye Sensitization of Nanocrystalline Tin Oxide by Perylene Derivatives, J. Phys. Chem. B 101, 4490–4493.

[27]. Chopra,K.; Major,S.; Panda,D. (1983): “Transparent Conductors—A Status Review,” Thin Solid Films 102, 1–46.

[28]. Wang,Y.D.; Ma,C.I.; Sun,X.D.; Li,H.D. (2001): "Synthesis of supramolecular-templated mesostructured tin oxide", Inorganic Chem. Commun. 4, 223–226.

[29]. Qi,L.;Ma,J.; Cheng,H.; Zhao,Z. (1998): Synthesis and characterization of mesostructured tin oxide with crystalline walls, Langmuir 14, 2579–2581.

[30]. Cullity, (1956): Elements of X-ray Diffraction, Addison-Wesley Publishing Co, Boston.

[31]. Zou,G.L.;Liu,R.;Chen,W.X.;Xu,Z.D. 2007): “Preparation and characterization of lamellar-like $Mg(OH)_2$ nanostructures via natural oxidation of Mg metal in formamide/water mixture,” Materials Research Bulletin, vol. 42, no. 6, pp. 1153–1158.

[32]. Zhang,J.; Gao,L. (2004): “Synthesis and characterization of nanocrystalline tin oxide by sol-gel method,” Journal of Solid State Chemistry, vol. 177, no. 4-5, pp. 1425–1430.

[33]. Jagriti Pal, Pratima Chauhan, (2009): Structural and optical characterization of tin dioxide nanoparticles prepared by a surfactant mediated method, Materials Characterization 60, 1512-1516.

[34]. Gnanam,S.; Rajendran,V. (2010) : Luminescence Properties of EG-Assisted SnO_2 nanoparticles by Sol-Gel Process Digest Journal of Nanomaterials and Biostructures 5: 699-704.

[35]. Gnanam S, Rajendran V (2010): Anionic, cationic and non-ionic surfactants-assisted hydrothermal synthesis of tin oxide nanoparticles and their photoluminescence property. Digest Journal of Nanomaterials and Biostructures 5: 623-628.

[36]. Mills,G.; Li,Z.G.; Meisel,D. (1988): “Photochemistry and spectroscopy of colloidal arsenic sesquisulfide,” Journal of Physical Chemistry, vol. 92, no. 3, pp. 822–828.

[37]. Bagheri.M.M.;Mohagheghia,b.;Shahtahmasebia,N.;Alinejada,M.R.;Youssefic,A.; Shokooh-Saremid,M. (2008): "The effect of the post-annealing temperature on the nano-structure and energy band gap of SnO_2 semiconducting oxide nano-particles synthesized by polymerizing–complexing sol–gel method", Physica B, Vol.403,pp. 2431–2437.

[38]. Cai,D.; Su,Y.; Chen,Y.Q; Jiang,J.; He,Z.Y.; Chen,L. (2005): Synthesis and photoluminescence properties of novel SnO_2 asterisk-like nanostructures, Mater. Lett. 59, 1984-1988.

[39]. Gu,F.; Wang, S.F.; Lv,M.K.; Qi,Y.X.; Zhou,G.J.; Xu,D.; Yuan,D.R. (2003): Luminescent properties of Mn^{2+}-doped SnO_2 nanoparticles, Inorg. Chem. Commun. 6, 882-885.

[40]. Hu, JQ.; Ma, XL.; Shang, NG.; Xie, ZY.; Wong, NB.; Lee, CS. et al. (2002): Large-scale rapid oxidation synthesis of SnO_2 nanoribbons. J Phys Chem B, 106:3823–3826.

[41]. Hu JQ, Bando Y, Liu QL, Golberg D. (2003): Laser ablation growth and optical properties of wide and long single-crystal SnO_2 nanoribbons. Adv Funct Mater 13:493–496.

[42]. Calestani D, Lazzarini L, Salviati G, Zha M.(2005): Morphological, structural and optical study of quasi-1D SnO2 nanowires and nanobelts. Cryst Res Technol. 40 ; 937–941.

[43]. Fagila G, Baratto C, Sberveglieri G, Zha M, Zappettini A. (2005): Adsorption effects of NO_2 at ppm level on visible photoluminescence response of SnO_2 nanobelts. Appl Phys Lett. 86:011923.
[44]. Maestre D, Cremades A, Piqueras J. (2005): Growth and luminescence properties of micro- and nanotubes in sintered tin oxide. J Appl Phys. 97:044316